Localization in strongly chaotic systems

1997 J. Phys. A: Math. Gen. 30 3603

(http://iopscience.iop.org/0305-4470/30/10/032)

J. Phys. A: Math. Gen. **30** (1997) 3603–3612. Printed in the UK PII: S0305-4470(97)81402-3

Localization in strongly chaotic systems

Mario Feingold

Department of Physics, Ben-Gurion University, Beer-Sheva 84105, Israel

Received 29 January 1997, in final form 19 March 1997

Abstract. We discuss the differences and similarities in structure between Hamiltonian matrices of strongly chaotic time-independent systems and the evolution operator matrix for the kicked-rotor model. Since the eigenvectors of the latter are exponentially localized, we study the influence of the differences between the two systems on this property. In particular, the Wigner ensemble is used to show that, for $\overline{h} \to 0$, the effect of the slow variation of the diagonal matrix elements in the Hamiltonian matrices is restricted to the tails of the eigenvectors.

1. Introduction

The quantum mechanical behaviour of strongly chaotic systems [1] is commonly thought to be of two apparently different types. On the one hand, there is the kicked rotor at large nonlinearity for which the eigenstates of the one-period evolution operator, U, are exponentially localized [2]. Due to localization, there is no repulsion between most levels and the spectrum of quasi-energies is characterized by a Poisson spacings distribution [3]. On the other hand, one has the strongly chaotic time-independent systems, e.g. the coupled quartic oscillators for some values of the parameters [4], where eigenstates in a phase-space representation are, on average, homogeneously spread over the corresponding energy shell. Such states are regarded as extended, leading to strong level repulsion and a Wigner spacings distribution [5]. We show in what follows that in ordered representations† there are similarities between the evolution matrix of the kicked rotor, U_{nm}, and the Hamiltonian matrix of strongly chaotic autonomous systems, H_{nm}. In particular, both matrices are banded and have some degree of randomness in their elements. On the other hand, one can also identify three qualitative differences between the two matrices: (1) the diagonal elements of H_{nm} vary slowly unlike those of U_{nm} that have constant absolute value, (2) the bandwidth of H_{nm} also varies while it is constant for U_{nm} and (3) an efficient mechanism that randomizes the matrix elements of U_{nm} through the use of two incommensurate numbers is absent in the H_{nm} matrix. It is the purpose of this paper to study the influence of the first difference on the behaviour of the eigenvectors and their localization properties. To this end we use the Wigner ensemble of banded random matrices with linearly growing diagonal elements whose structure interpolates between that of the U_{nm} matrix and that of the H_{nm} one. Specifically, the Wigner ensemble models a U_{nm} matrix to which a simplified version of the first difference has been added. This approach enables us to separate the effect of the first structural difference on the localization properties of the eigenvectors from the effects of the other two.

† Ordered bases are composed of eigenvectors of some operator which are arranged in increasing order of the corresponding eigenvalues.

0305-4470/97/103603+10$19.50

A notable difficulty in generalizing the concept of localization to arbitrary bases is the extent to which the result of this generalization is distinct from the obvious effect of perturbative localization. In other words, it is clear that in a basis that is composed of the eigenvectors themselves or of eigenvectors of an operator that is close to H, $H + \epsilon V$, only a few of the vector components will be significantly different from zero and, moreover, if the basis is ordered, these will be tightly clustered. However, we show in what follows that, for fixed ϵ, one can always find a small enough value of $\overline{h}$, $\overline{h}_\epsilon$, for which perturbation theory is bound to fail and, therefore, our study is mostly focused on localization in the non-perturbative regime, $\overline{h} < \overline{h}_\epsilon$. In fact, the Wigner ensemble, unifies the descriptions of both the perturbative and the non-perturbative regimes and also of the transition between the two into a single model.

It is worthwhile to point out that the physical role of the evolution operator in the case of the kicked rotor is different from that of the Hamiltonian in a time independent system. However, since the kicked rotor can be mapped onto an Anderson model whose Hamiltonian is closely related to the evolution matrix of the kicked rotor, we believe that this difference will not affect any of our conclusions. An alternative argument for ignoring the physical role of the U_{nm} and H_{nm} matrices is that, in fact, our analysis of the corresponding eigenvectors only relies on the structure of these matrices and the behaviour of their matrix elements.

This paper is organized as follows. In order to emphasize the similarities and differences between the U_{nm} and H_{nm} matrices, in the next section we review the relevant properties of the kicked rotor and of strongly chaotic autonomous Hamiltonians. In section 3, we present the Wigner ensemble and the known properties of its local density of states, $\rho_L(E, n)$. We then establish the relation between $\rho_L(E, n)$ and the shape of the corresponding eigenvectors. The average eigenvector of the coupled quartic-oscillators model is compared with that of the Wigner ensemble in section 4. We find poor agreement between the two, suggesting that the variation of the bandwidth and the correlations in the H_{nm} matrix have significant effects on the eigenvectors. Qualitatively, however, far within the non-perturbative regime, the eigenvectors of this model rapidly decay away from the maximum showing, for the first time, evidence of non-exponential localization in strongly-chaotic autonomous Hamiltonians. The conclusions are presented in section 5.

2. Structure of matrices

Most of the material in this section has appeared before in various papers [2, 6, 7] and is reviewed here in order to introduce the necessary notation and to assist the reader. However, equation (6) was previously incorrectly stated and here we present a modified derivation that is new. On one side of our comparison we have the kicked rotor

$$H = \frac{p^2}{2} + V(q) \sum_{n=-\infty}^{\infty} \delta(t - nT) \tag{1}$$

where T is the period of the kicks and $V(q) = k \cos q$, which can be mapped onto an Anderson model for the motion of an electron on a purely one-dimensional disordered lattice. This mapping implies that the eigenvectors of the corresponding one-period evolution operator, U_{nm}, in the basis of momentum states are exponentially localized. A more direct approach to understanding localization is based on the structure of the U_{nm} matrix

$$U_{nm} = \exp(-\mathrm{i}\overline{h}Tn^2/2)(-\mathrm{i})^{m-n} J_{m-n}(k). \tag{2}$$

First, it is banded due to the decay of the Bessel functions, J_{m-n}, as their index grows. Secondly, for large enough n's and values of $\overline{h}T$ that are incommensurate with π, the phases

of the matrix elements in equation (2) are quite close to being uncorrelated random numbers. Accordingly, the eigenvectors of U_{nm} are expected to behave similarly to those of a banded random matrix [8] of the same bandwidth, b. Since the latter can be analysed using a transfer-matrix formalism, the eigenvectors are exponentially localized with a localization length, ξ, that is proportional to b^2, $\xi = \gamma b^2$ [7–9].

The kicked rotor was originally introduced as a simplified but representative Poincaré map of a time-independent system with two degrees of freedom, $d = 2$, also known as the standard map. It is, therefore, also natural to expect that its quantum mechanics should be reminiscent of that of time-independent systems. One obstacle that has prevented the search for this similarity is the fact that eigenstates of time-independent systems are best understood in phase-space representations through the Berry–Voros conjecture [1]. However, in order to obtain an analogous description to that leading to the banded evolution operator, U_{nm}, a basis with a natural ordering is required. Let $H = H_0 + V$ be an arbitrary separation of H and $\overline{h}$ be small. Using the eigenvectors of H_0, v_n, arranged in increasing order of the corresponding eigenvalues, $E_{0,n}$, one obtains for H a matrix representation, H_{nm}, that is banded and, moreover, has diagonal elements which vary on classical energy scales. The latter feature that is related to energy conservation is absent in the U_{nm} matrix where diagonal elements are of constant absolute value (see equation (2)). On the other hand, the simple mechanism that generates randomness in the U_{nm} matrix is absent in the case of H_{nm}, making the latter significantly less random. This is a direct consequence of the fact that while H_0 appears in the exponent in the U_{nm} matrix, in the H_{nm} matrix it is simply added to V.

We now turn to describe the structure of the H_{nm} matrix. Let us assume that all the relevant operators, namely, H, H_0 and V, are well-behaved functions of the canonical variables, $\boldsymbol{z} \equiv (\boldsymbol{q}, \boldsymbol{p})$. Then, under quite general conditions, it is known [10] that the energy average of the diagonal elements is equal to the corresponding microcanonical average, that is

$$\langle H_{nn} \rangle = \{H(\boldsymbol{z})\}_{E_{0,n}} \tag{3}$$

where for any function, $F(\boldsymbol{z})$,

$$\{F(\boldsymbol{z})\}_{E_0} \equiv \frac{\int \mathrm{d}\boldsymbol{z}\, F(\boldsymbol{z}) \delta[E_0 - H_0(\boldsymbol{z})]}{\int \mathrm{d}\boldsymbol{z}\, \delta[E_0 - H_0(\boldsymbol{z})]}. \tag{4}$$

Moreover, for real Hamiltonian matrices the variance of the diagonal elements, $\sigma_D^2 \equiv \langle H_{nn}^2 \rangle - \langle H_{nn} \rangle^2$, was shown [11] to be equal to twice the variance of the off-diagonal matrix elements that are close to the diagonal, σ_O^2, and correspondingly, $\sigma_D^2 = \mathrm{O}(\overline{h}^{d-1})$. Therefore, in the semiclassical limit the distribution of diagonal elements has vanishing width whenever $d > 1$. As we now show, this fact is extremely helpful in understanding the behaviour of the off-diagonal matrix elements of H_{nm}. In the nth row of H_{nm}, the average distance of matrix elements from the diagonal measured in units of energy is

$$(\Delta E_{0,n})^2 \equiv \frac{\sum_m (E_{0,m} - E_{0,n})^2 |H_{nm}|^2}{\sum_{m(\neq n)} |H_{nm}|^2} = -\frac{([H_0, H]^2)_{nn}}{(H^2)_{nn} - (H_{nn})^2} \tag{5}$$

and using equation (3)

$$\langle (\Delta E_{0,n})^2 \rangle \to \overline{h}^2 \frac{\{[H_0, H]^2_{\mathrm{PB}}\}}{\{H^2\} - \{H\}^2} \qquad \text{for } \overline{h} \to 0 \tag{6}$$

where the commutator of equation (5) was replaced by $\mathrm{i}\overline{h}$ times the corresponding Poisson bracket, $[\ldots]_{\mathrm{PB}}$. Notice that while equation (3) holds for arbitrary values of $\overline{h}$, equation (6)

only applies for small enough $\overline{h}$. The reason is that in equation (6), the l.h.s. is the average of a ratio of diagonal elements which, in general, differs from the ratio of the averages on the r.h.s. However, if $d > 1$ and $\overline{h} \to 0$, then the width of the distribution of the diagonal elements appearing in the denominator of equation (5) becomes vanishingly small and, therefore, these elements play the role of constants in the averaging.

In order to fully grasp the implications of equation (6), it is necessary to express $\langle(\Delta E_{0,n})^2\rangle^{1/2}$ in terms of the number of states by multiplying it with the mean density of states, $\rho(E_0)$, which is $O(\overline{h}^{-d})$, such that $\langle(\Delta N_{0,n})^2\rangle^{1/2} = O(\overline{h}^{1-d})$. On the one hand, for $d > 1$ and $\overline{h} \to 0$, $\langle(\Delta N_{0,n})^2\rangle^{1/2}$ diverges. On the other hand, however, the number of states in any classical energy range which, in turn, corresponds to the size of the truncated Hamiltonian matrix, N, is $O(\overline{h}^{-d})$ and, therefore, diverges much faster than the bandwidth. In fact, $\langle(\Delta N_{0,n})^2\rangle^{1/2}/N = O(\overline{h})$ and accordingly, for small enough $\overline{h}$, the H_{nm} matrix is banded. Moreover, equation (3) implies that the diagonal matrix elements, H_{nn}, vary on average as the volume of the energy shell changes. Both these features are absent in the traditional random matrix ensembles, e.g. the Gaussian orthogonal ensemble (GOE), and this lack of structure leads to extended eigenvectors. A random matrix model which does include a simplified version of this structure is the Wigner ensemble [7, 12] which is described in the next section.

3. The Wigner ensemble

The Wigner ensemble is composed of banded random matrices of band width, b, with diagonal elements that, on average, form a ladder of constant spacings, α. Namely $\langle h_{nm}\rangle_e = \alpha n \delta_{nm}$, where h_{nm} is the matrix element of the Wigner ensemble and $\langle\ldots\rangle_e$ denotes averaging over the ensemble. Moreover, $\sigma_{nm}^2 \equiv \langle h_{nm}^2\rangle_e - \langle h_{nm}\rangle_e^2 = 1 + \delta_{nm}$ for $|n - m| < b$ and vanishes otherwise. As in the case of the GOE, the matrix elements are uncorrelated Gaussian distributed random variables.

For $\alpha = 0$ the Wigner ensemble is equivalent to the banded random matrix ensemble (BRME) [8] which in turn can be thought of as an Anderson model [13] with random, long-range hopping. Similarly, it is useful to interpret the Wigner ensemble at finite α as an Anderson model under the influence of a constant electric field of strength α. This approach enables one to visualize the behaviour of the local density of states which is closely related to that of the eigenvectors.

In the absence of an electric field, the Anderson model is, on average, translational invariant. Therefore, the ensemble-averaged local density of states,

$$\rho_L(E, n) \equiv \left\langle \sum_i |u_i(n)|^2 \delta(E - E_i) \right\rangle_e \tag{7}$$

where $u_i(n)$ is the nth component of the ith eigenvector of the random matrix and E_i the corresponding eigenvalue, is proportional to the average density of states itself, $\rho(E)$. In particular, for the BRME, both $\rho(E)$ and $\rho_L(E, n)$ are in the form of a semicircle of radius $2\sqrt{2b}$. While turning on the electric field breaks the translational invariance, for small enough fields the hopping potential varies much faster than the electric one and the adiabatic approximation that relies on the separation of these two energy scales is known as the *sloping-band picture* [9]. In this regime, one expects that at each site the $\rho_L(E, n)$ is similar to the one at zero field apart from its centre being shifted to include the additional electric energy which increases linearly along the lattice. This is schematically illustrated in figure 1 where the allowed region inside the band represents the energy shell of the Wigner ensemble. While taking a section through the energy band at a fixed position, n, gives the

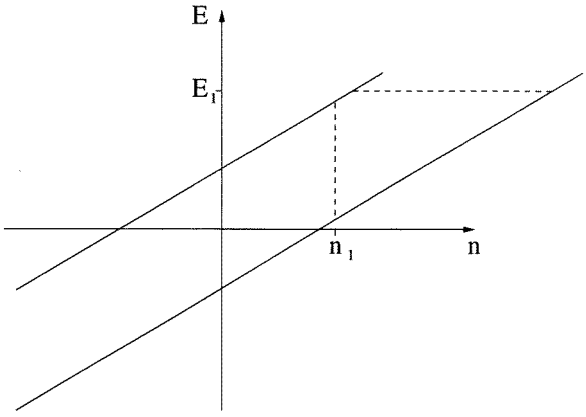

Figure 1. The sloping-band picture for the local density of states. The full lines correspond to the energy band edges. The broken lines indicate a fixed n section which gives the distribution of the local energies and a fixed energy section which for small q is equivalent to the average eigenvector.

distribution of the local energies, a section at a fixed energy is expected to give information on the behaviour of the average eigenvector. In particular, one expects that the average eigenvector is constrained to lie within the energy shell. Independently of the sloping-band picture, the $\rho_L(E,n)$ for the Wigner ensemble was derived in [12] (see also [14–16]). It was found that

$$\rho_L(E,n) = \frac{1}{\alpha b} f\left(\frac{E-\alpha n}{\alpha b}, q\right) \tag{8}$$

where $q \equiv (\alpha^2 b)^{-1}$. For small electric fields, $q \gg 1$, the semicircle behaviour persists

$$f(x,q) = (4\pi q)^{-1}\sqrt{8q - x^2} \tag{9}$$

and for large fields, $q \ll 1$, the profile is Lorentzian,

$$f(x,q) = \frac{q}{\pi^2 q^2 + x^2}. \tag{10}$$

In fact, equations (9) and (10) only hold for $x < 1$. For $x \gg 1$, f is the solution of an integral equation for which

$$f(x,q) \simeq c \exp\left[-2x \ln\left(xe^{-1}\sqrt{2q^{-1}\ln(x/\sqrt{q})}\right)\right] \tag{11}$$

represents an approximate solution [17]. Another approximation leading to equations (10) and (11), where the discrete index of the matrix is replaced by a continuous variable, fails when α becomes of order unity. The behaviour of $\rho_L(E,n)$ in the limit $\alpha \gg 1$ was also studied [14]. Finally, it is important to stress that the $q \ll 1$ regime is of a perturbative nature and all the corresponding results can be obtained using a perturbation expansion in the strength of the hopping potential.

We now discuss the behaviour of the average eigenvector, which is defined as the average variance of the vector component at a fixed distance from the largest component, $g(l) \equiv \langle |u_i(n-n_{\max})|^2 \rangle_E$, where $l \equiv n - n_{\max}$ and $\langle \ldots \rangle_E$ denotes averaging over both energy and the ensemble. Moreover, $n_{\max}$ is the index of the largest component of the ith vector and ignoring finite N effects $\langle n_{\max}(i) \rangle_e = i$. We find that the tails of $g(l)$ far outside the

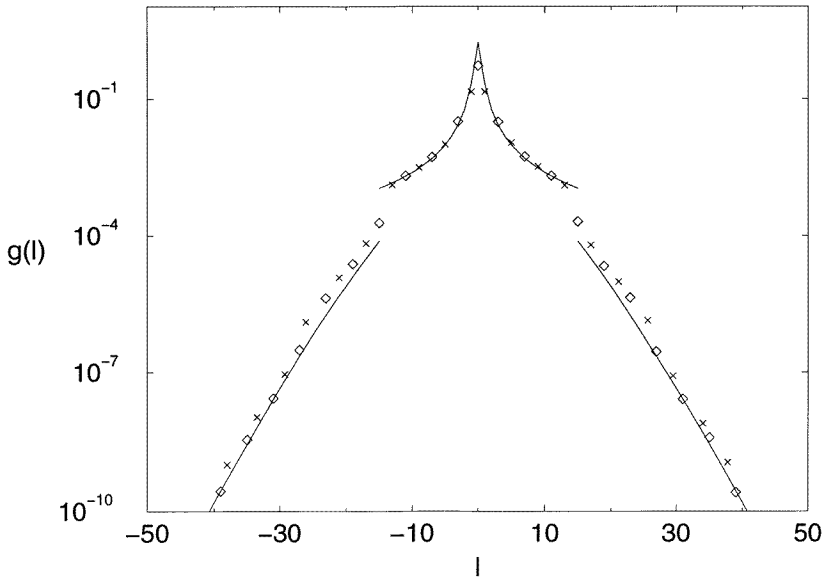

Figure 2. The numerically obtained $g(l)$ function for the Wigner ensemble with $\alpha = 2$ and $b = 14$ ($q = 0.0179$) ($\diamond$) is compared with equations (10)–(12) (full curves). Moreover, the $\times$ symbols represent the numerical $\frac{1}{4}g(l/4)$ function for the Wigner ensemble with $\alpha = 1$ and $b = 56$ (same q), verifying the scaling of equation (12).

energy shell are directly determined by the local density of states, $\rho_L(E, n)$, (see figure 2) in the sense that

$$g(l) = \frac{1}{b} f\left(\frac{l}{b}, q\right). \tag{12}$$

As was shown in [17], this directly follows from the fact that perturbation theory gives the same integral equation for $g(l)$ at $l \gg b$ as was found by Wigner [12] for the asymptotic tails of $\rho_L(E, n)$. On the other hand, inside the energy shell the shape of $g(l)$ is different in the large and small q regimes. At large electric field, $q \ll 1$, the disorder is too weak to localize the eigenvector and accordingly, as in the case of the tails, $g(l)$ is determined by the local density of states through equation (12) taking on Lorentzian form. For weak field, however, $q \gg 1$, the band is only slightly sloped and, as a consequence, the variation of the local density of states is slower than the scale on which localization due to disorder takes place. Thus, the disorder is dominant and in the $q \to \infty$ limit the same exponentially localized shape as in the absence of the electric field is obtained (see figure 3) [18]. The transition between the two regimes is centred at q_c where the hopping range is of the same size as the spatial energy-shell width. A rough estimate of q_c can be obtained assuming that the width of the energy shell does not change with α staying $4\sqrt{2b}$ all the way down to q_c. While such an estimate gives $q_c \approx 0.125$, numerically a value of $q_c \simeq 0.09$ is obtained [15].

In order to establish the correspondence between the various regimes of the Wigner ensemble and the structure of Hamiltonian matrices, one needs to use the semiclassical formulae for the parameters of the ensemble. Notice that the variances of the matrix elements in the Wigner ensemble are O(1) unlike those in H_{nm} and, therefore, the effective value of the electric field for the Hamiltonian matrix is $\alpha_{\text{eff}} = \alpha/\sigma_O$. Accordingly, from equations (3)–(6) one obtains $q = \mathrm{O}(\overline{h}^{-2})$ implying that, in the semiclassical limit, the H_{nm}

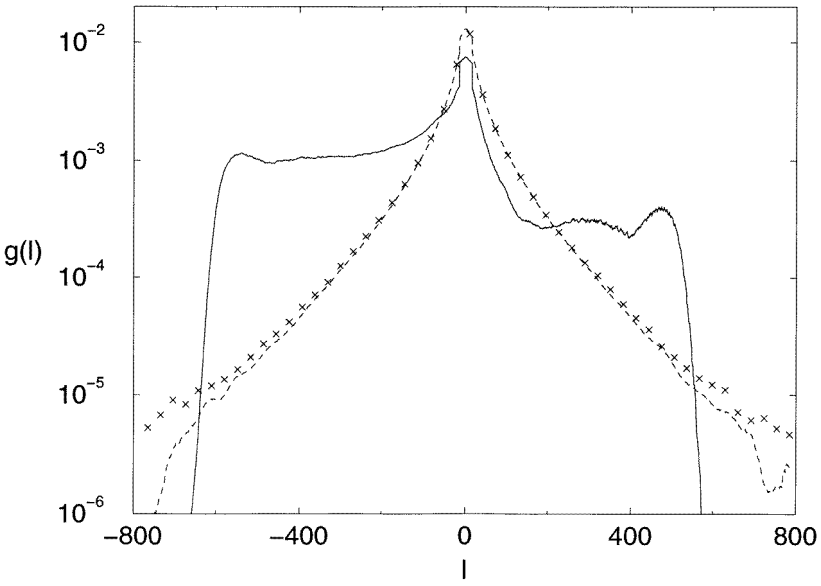

Figure 3. The average eigenvector for the coupled quartic oscillators (full curve) is compared with the corresponding result from the Wigner ensemble (broken curve). The × symbols correspond to the $g(l)$ of the Wigner ensemble with the same b but $\alpha = 0$, indicating that in this regime, α has almost no influence on the shape of the average eigenvector except for the sharp drop at $l \approx \pm 670$ due to the energy-band edge. In order to further reduce statistical fluctuations, the curves in this figure have been smoothed using a running average over 30 neighbouring sites.

matrices are in the disorder-dominated non-perturbative regime. Moreover, the fraction of the eigenvector that is not influenced by the local density of states, that is, the part lying within the energy band, extends over a range of sites that is $O(\sqrt{b}\alpha^{-1}) = O(\overline{h}^{-d})$ which also diverges when $\overline{h} \to 0$. *Accordingly, the Wigner ensemble suggests that for small* $\overline{h}$ *the influence of the diagonal elements of* H_{nm} *on the shape of its average eigenvectors is restricted to the far away tails. Aside from these tails, the extent to which the eigenvectors of* H_{nm} *resemble those of the kicked-rotor evolution matrix is controlled by the energy variation of the bandwidth and the amount of correlations in the* H_{nm} *matrix.* This is the main result of the paper. Finally, notice that the spatial width of the energy band is determined by a classical energy range, δE_0. This is the range of energy values of H_0 for which the corresponding energy shells intersect the $H(z) = E$ energy shell of H. While for the Wigner ensemble δE_0 is constant, in a generic Hamiltonian model it will vary with E.

4. The coupled quartic oscillators

Let us now examine the extent to which the Wigner ensemble is a good model for a particular Hamiltonian matrix. Such a study has been previously performed in [17] using a model of the Ce atom that is quite complicated. In particular, it has 12 degrees of freedom corresponding to four electrons in three dimensions. Moreover, no analysis of the classical dynamics was made for this model and, consequently, islands of regular motion could influence the structure of the Hamiltonian matrix. Despite these apparent drawbacks, the authors find good agreement with the prediction of the corresponding Wigner ensemble

for the eigenvector tails outside the energy shell. On the other hand, the value of q that they find is close to q_c, namely $q \simeq 0.18$. While this is probably due to the fact that their value of $\bar{h}$ is relatively large, it is not far enough from the transition in order to obtain the behaviour of the eigenvectors in the disorder-dominated regime. In fact, in [17] the authors have tried to fit the shape of the eigenvectors inside the energy shell to Lorentzians and, as expected, found poor agreement. Further analysis of the Ce atom eigenvectors showed [19] that for a global quantity, namely the average localization length the agreement to the corresponding Wigner ensemble is better than 5% and roughly within the estimated error bars of the calculation.

In order to have better control over the properties of the model, we study the coupled quartic oscillators Hamiltonian,

$$H = \frac{p_1^2 + p_2^2}{2} + b_c q_1^4 + b_c^{-1} q_2^4 - a_k q_1^2 q_2^2. \tag{13}$$

For $b_c = \pi/4$ and $a_k = 1.6$ we find that the classical dynamics in the Poincaré section appears to be fully chaotic to a resolution of about 0.4% of $\bar{h}$ which, in turn, was taken to be unity. The basis we choose for this study is both the simplest possible and the most widely used in physical applications, namely that of harmonic oscillators. In other words, we let H_0 be composed of two uncoupled harmonic oscillators with frequencies $w_1 = 4.11$ and $w_2 = 1.3$. We then truncate the resulting H_{nm} matrix to the first N basis states, $N = 800$, and calculate the average parameters obtaining $\alpha_{\text{eff}} = 0.013$ and $b = 12.9$. Accordingly, $q = 446 \gg q_c$ and the matrix is far in the disorder-dominated regime. In figure 3 we show the corresponding $g(l)$ function as obtained from averaging over all the eigenvectors†. The prediction of the Wigner ensemble that has the same α and $b = 13$ is quite close to the numerically obtained $g(l)$ in the neighbourhood of the maximum up to $l \approx \pm 100$. Further away, however, the Hamiltonian $g(l)$ saturates into broad shoulders that are absent in the case of the Wigner ensemble leading to significant disagreement between the two shapes. This saturation is reminiscent of the behaviour observed for the eigenvectors of the U_{nm} matrix in the limit of small $\tau \equiv \bar{h}T$ where its matrix elements are strongly correlated (see equation (2) and figure 8 in [20]). A more detailed study is necessary in order to verify whether the saturation of the $g(l)$ is indeed a consequence of enhanced correlations in the H_{nm} matrix and we postpone it for future work. On the other hand, it is natural to assume that the asymmetry with respect to $l = 0$ in the Hamiltonian $g(l)$ is due to the energy variation of the matrix bandwidth distinguishing between the inside and the outside of the energy shell. Finally, at $l_+ \approx 470$ and $l_- \approx -540$ the saturation shoulders abruptly end in a sharp drop which represents the sole effect of the diagonal elements. The values of l where the tails of the Wigner $g(l)$ begin are of the same order as those for the Hamiltonian $g(l)$. The lack of better agreement is due to the fact that in the Hamiltonian case the energy shell width varies with energy and, therefore, in some range close to $l_\pm$ the averaging mixes regions which are inside the energy shell with regions that are outside.

† On the one hand, only $f \approx 22\%$ of the eigenvalues of the $N \times N$ block are converged within 1% and for a similar fraction of the individual eigenvectors the first fN components are equally accurate. We obtain f by comparing the eigenvalues and eigenvectors resulting from two different values of N, 800 and 1000. On the other hand, the truncation errors in the eigenvectors were found to average away such that, practically, $g(l)$, does not depend on N. Accordingly, we use the entire block in computing $g(l)$. Since the Wigner ensemble itself mimics the structure of a finite block that is part of a typically infinite matrix, this approach further tightens the analogy between the random-matrix model and the Hamiltonian system.

5. Conclusions

In summary, our findings suggest that although eigenvectors of time-independent Hamiltonian systems are localized inside the energy shell in the $\bar{h} \to 0$ limit, the quantitative behaviour is controlled by the degree of correlation between matrix elements and by the energy variation of the bandwidth. The way in which these two effects influence the structure of the eigenvectors is an exciting open question to be addressed in future work. In order to distinguish between the influence of the correlations and that of the bandwidth variation one should unfold the structure of the Hamiltonian matrix in a way analogous to the unfolding of the spectrum prior to analysing the statistics of its fluctuations. In particular, the band should be stretched in the rows where it is smaller than the average and compressed when it is larger. Moreover, the diagonal elements should be unfolded to follow the best fitting straight line and the off-diagonal elements should be normalized to be, on average, of unit variance. The resulting matrix will have the same structure as the members of the Wigner ensemble with the addition of the correlations of a Hamiltonian matrix. On the other hand, one expects that as the basis we use becomes more complex there will be less correlations in the Hamiltonian matrix. One particularly interesting way of increasing the complexity of the basis is to choose H_0 such that its classical dynamics is strongly chaotic rather than fully integrable as in the present study.

The results of this work are important for a wide variety of physical problems. For example, finding the shape of eigenvectors for a large class of bases would allow for a statistical analysis of the corresponding dynamics. Moreover, by analogy with the localization of electrons on random lattices, the localization of eigenvectors in time-independent Hamiltonian systems is expected to affect the conductance properties of mesoscopic quantum dots [21]. In contrast to the case of the eigenvectors, the eigenvalue statistics are greatly influenced by the behaviour of the diagonal matrix elements. Specifically, a finite α makes neighbouring eigenvalues correspond to eigenvectors that strongly overlap and the ensuing level repulsion leads to a Wigner spacings distribution. Quantitatively, however, the spacings distribution for the Wigner ensemble was found [7] to depend on a basis dependent scaling variable, $y = \alpha b^{3/2}$, and this fact casts serious doubts as to whether this ensemble can be used to model the spectral properties of Hamiltonian systems.

Acknowledgments

We thank B Horovitz, D M Leitner, B Shapiro and M Wilkinson for useful discussions. This work was supported by the Israel Science Foundation administered by the Israel Academy of Sciences and Humanities.

References

[1] Berry M V 1983 *Chaotic Behaviour of Deterministic Systems* vol 36, ed G Iooss, R H G Helleman and R Stora (Amsterdam: North-Holland) p 172
[2] Fishman S, Grempel D R and Prange R E 1982 *Phys. Rev. Lett.* **49** 509
[3] Feingold M, Fishman S, Grempel D R and Prange R E 1985 *Phys. Rev.* B **31** 6852
[4] Seligman T H, Verbaarschot J J M and Zirnbauer M R 1985 *J. Phys. A: Math. Gen.* **19** 2751
[5] Bohigas O and Giannoni M J 1984 *Mathematical and Computational Methods in Nuclear Physics (Lecture Notes in Physics 209)* ed J S Dehesa, J M G Gomez and A Polls (Berlin: Springer) p 1
[6] Feingold M, Leitner D M and Piro O 1989 *Phys. Rev.* A **39** 6507
[7] Feingold M, Leitner D M and Wilkinson M 1991 *Phys. Rev. Lett.* **66** 986

Feingold M, Leitner D M and Wilkinson M 1991 *J. Phys. A: Math. Gen.* **24** 175
[8] Casati G, Molinari L and Izrailev F 1990 *Phys. Rev. Lett.* **64** 1851
[9] Fyodorov Y V and Mirlin A D 1991 *Phys. Rev. Lett.* **67** 2405
[10] Shnirelman A I 1974 *Usp. Mat. Nauk.* **29**/6 181
Feingold M, Moiseyev N and Peres A 1985 *Chem. Phys. Lett.* **177** 344
[11] Feingold M and Peres A 1986 *Phys. Rev.* A **34** 591
[12] Wigner E P 1955 *Ann. Math.* **62** 548
Wigner E P 1957 *Ann. Math.* **65** 203
[13] Ishii K 1973 *Suppl. Prog. Theor. Phys.* **53** 77
[14] Leitner D M and Feingold M 1993 *J. Phys. A: Math. Gen.* **26** 7367
[15] Casati G, Chirikov B V, Guarneri I and Izrailev F M 1993 *Phys. Rev.* E **48** 1613
[16] Fyodorov Y V, Chubykalo O A, Izrailev F M and Casati G 1996 *Phys. Rev. Lett.* **76** 1603
[17] Flambaum V V, Gribakina A A, Gribakin G F and Kozlov M G 1994 *Phys. Rev.* A **50** 267
[18] Parts of this picture were independently suggested by Casati G, Chirikov B V, Guarneri I and Izrailev F M 1995 *Preprint*
[19] Feingold M and Piro O 1995 *Phys. Rev.* A **51** 4279
[20] Grempel D R, Prange R E and Fishman S 1984 *Phys. Rev.* A **31** 1639
[21] Beenakker C W J and van Houten H 1991 *Solid State Phys.* vol 44, ed H Ehrenreich and D Turnbull (New York: Academic) p 1